

SPC25 promotes hepatocellular carcinoma metastasis via activating the FAK/PI3K/AKT signaling pathway through ITGB4

WEN-KAI SHI^{1*}, QIAO-LI SHANG^{2*} and YONG-FU ZHAO¹

¹Department of Hepatopancreatobiliary Surgery, The First Affiliated Hospital of Zhengzhou University, Zhengzhou, Henan 450052; ²The Seventh Plastic Department, Plastic Surgery Hospital, Chinese Academy of Medical Sciences and Peking Union Medical College, Beijing 100144, P.R. China

Received December 15, 2021; Accepted February 25, 2022

DOI: 10.3892/or.2022.8302

Abstract. Hepatocellular carcinoma (HCC) is a malignant tumor with a high metastatic rate. Recent studies have shown that the mitosis-associated spindle-assembly checkpoint regulatory protein spindle pole body component 25 homolog (SPC25) promotes HCC progression, although the underlying mechanism has yet to be fully elucidated. The aim of the present study was to investigate the mechanism through which SPC25 may promote HCC progression in greater detail. First, the expression of SPC25 was analyzed in publicly available databases to explore the association between SPC25 and HCC metastasis. Western blotting was subsequently performed to examine the level of SPC25 expression in different HCC cell lines. SPC25 was then silenced in HCCLM3 and Huh7 cells, and the effects of SPC25 silencing were investigated using cell proliferation, wound-healing, Transwell migration assays and an *in vivo* mouse model. Finally, the mechanism of SPC25 action with respect to the promotion of HCC metastasis was explored using microarray analysis and rescue experiments. The results obtained demonstrated that SPC25 is highly expressed in HCC, and this high level of expression is associated with poor prognosis and metastasis. Moreover, SPC25 silencing led to a marked inhibition of the invasion and migration of HCC cells both *in vitro* and *in vivo*. The gene-expression profiling and mechanistic experiments suggest that SPC25 preferentially influences the expression of genes associated with extracellular matrix (ECM)-integrin interactions, including integrin subunit $\beta 4$ (ITGB4), an upstream element of

the integrin pathway. ITGB4 upregulation partly reversed the decline in cell invasion and migration capacities that resulted from SPC25 silencing. Furthermore, deleting both SPC25 and ITGB4 caused a decrease in the phosphorylation of focal adhesion kinase (FAK), phosphoinositide 3-kinase (PI3K) and AKT, which are downstream elements of the integrin pathway. Taken together, the results of the present study demonstrated the important role of SPC25 as a prognostic indicator and as a promoter of metastasis in HCC, and the underlying mechanism of its action has been partially elucidated, suggesting that SPC25 could be used as a biomarker and as a target for therapeutic intervention in the treatment of HCC.

Introduction

Liver cancer is an aggressive tumor, and its incidence is increasing globally (1). Hepatocellular carcinoma (HCC), accounting for more than 90% of the total cases of primary liver cancer, is the sixth most common type of cancer, and the fourth most common cause of cancer-associated deaths worldwide (2). The majority of patients are diagnosed at an advanced stage, at which time they have lost the opportunity of operable (surgical) therapy. For inoperable patients, the drugs that are available as molecular-targeting therapies include sorafenib and lenvatinib. However, sorafenib only extends the survival of patients by 3 months on average, and the objective response rate is only 2-3% (3); the extension of survival time of patients when administered lenvatinib are similar to those of sorafenib (4). The majority of patients with HCC already display metastasis at the time of diagnosis, even if their tumors are small. Complications due to tumor metastasis are the leading cause of cancer-associated deaths (5). Previous research published recently has shown that changes in gene expression, the tumor microenvironment and epithelial-to-mesenchymal transition (EMT) are associated with tumor metastasis (6), although the complexity of the underlying mechanism has only been partially elucidated for certain types of cancer. Consequently, a better understanding of the molecular mechanisms of HCC metastasis is urgently required in order to provide new opportunities for therapeutic interventions.

The extracellular matrix (ECM) is composed of interstitial collagens and basement membrane. In addition to providing

Correspondence to: Dr Wen-Kai Shi or Professor Yong-Fu Zhao, Department of Hepatopancreatobiliary Surgery, The First Affiliated Hospital of Zhengzhou University, No. 1 East Jianshe Road, Erqi District, Zhengzhou, Henan 450052, P.R. China
E-mail: shiwenkai@aliyun.com
E-mail: zhaoyongfu_doc@163.com

*Contributed equally

Key words: hepatocellular carcinoma, SPC25, metastasis, integrin subunit $\beta 4$

tissue structural integrity and scaffolding, ECM also adheres to the integrin family on cell membranes forming focal adhesions that serve to promote tumor metastasis (7). The interaction between laminin-332, one of the main proteins of the ECM, and integrin $\alpha 6\beta 4$ (ITGA6 and ITGB4) plays a key role in mediating the recognition and adhesion of cells with the ECM, and also with respect to signal transmission (8). Upon ligation, the integrin-mediated pathway is activated, and the integrin-mediated phosphorylation of focal adhesion kinase (FAK) activates downstream signaling (9). In particular, the hyperactivation of FAK, phosphoinositide 3-kinase (PI3K) and AKT has been shown to be a common occurrence in human malignancies, including esophageal squamous cell carcinoma, breast cancer and HCC, and is involved with tumor metastasis (10-12).

Spindle pole body component 25 homolog (SPC25) is a mitosis-associated spindle-assembly checkpoint regulatory protein (13) that is involved with genomic instability (14). SPC25 has been shown to be highly expressed in tumors, including prostate, breast and non-small cell lung cancer (NSCLC), and is associated with tumor progression (15-17). In previously published studies on HCC, the results revealed that SPC25 acts as an oncogene in HCC progression (18-20). However, the underlying mechanism has yet to be fully elucidated. In the present study, it was demonstrated that overexpression of SPC25 in HCC is associated with poor prognosis, and both *in vitro* and *in vivo* experiments were used to demonstrate the promotion of metastasis by SPC25. The results of Agilent cDNA microarray analysis showed that SPC25 silencing was significantly correlated with 'ECM receptor interactions' which were mainly mediated by the interaction of laminin-332 and integrin $\alpha 6\beta 4$ (ITGA6 and ITGB4). *ITGB4* and *SPC25* had the strongest positive correlation based on the TCGA data and PCR and had a similar role in promoting HCC metastasis. Ectopic overexpression of *ITGB4* with simultaneous silencing of SPC25 partially mitigated the reduction in cell invasion and migration capability caused by SPC25 silencing. In the KEGG enrichment analysis, we also found that the PI3K/AKT signaling pathway was significantly altered. Previous study has shown that integrin laminin binding increased FAK phosphorylation, which induces activation of the PI3K/AKT signaling pathway to promote tumor metastasis (10). The results of the present study revealed that *ITGB4* may be the main downstream mediator of SPC25-induced metastatic activity that is involved in ECM-integrin interactions, which subsequently activate the FAK/PI3K/AKT signaling pathway to promote metastasis in HCC.

Materials and methods

Tissue microarrays (TMAs) and immunohistochemistry (IHC) assay. The present study was approved by the Institutional Review Board of the First Affiliated Hospital of Zhengzhou University. All patients signed informed consent forms, and the study was performed in accordance with the principles dictated in the Declaration of Helsinki. TMAs were constructed with 141 pairs of HCC tumor and normal liver tissues, which were collected at our center between January 2012 and December 2015. The mean age of the patients was 53.4 years (25-77 years).

As described previously (21), immunohistochemistry (IHC) assay was performed using an UltraVision Quanto Detection System HRP (Thermo Fisher Scientific, Inc.) according to the manufacturer's instructions, and the SPC25 antibody (1:100; cat. no. ab121395; Abcam) was used, and incubation was performed at 4°C for 12 h. Subsequently, the integrated optical density (IOD) value was detected using Image-Pro Plus 6.0 software (Image-Pro Plus, http://scicrunch.org/resolver/SCR_007369; Media Cybernetics, Inc.).

Bioinformatics analysis based on public databases. The expression profile of liver cancer was obtained from The Cancer Genome Atlas (TCGA) database (<https://www.cancer.gov/tcga>) and The International Cancer Genome Consortium (ICGC) database (<https://dcc.icgc.org/>) and the gene expression profiles of GSE102079 (22) and GSE112790 (23) were downloaded from the Gene Expression Omnibus (GEO) database. Then the gene expression data for HCC and adjacent non-cancerous tissues were obtained. The Student's t-test was used to detect the differential expression of SPC25. Kaplan-Meier method was used to compare survival analysis for the SPC25 high and low expression patients based on the TCGA and ICGC database.

Cell culture. All HCC cell lines used (MHCC97H, MHCC97L, HCCLM3 and Huh7) and the immortalized human hepatocyte MIHA cells were obtained from the Liver Cancer Institute at Fudan University, and cultured in HyClone Dulbecco's modified Eagle's medium (DMEM) or RPMI-1640 medium (for MIHA) with high glucose (Cytiva), supplemented with 10% Gibco® fetal bovine serum (FBS) and 1% penicillin/streptomycin (Invitrogen; Thermo Fisher Scientific, Inc.) in an atmosphere of 5% CO₂ at 37°C. The cell lines were authenticated via STR profiling.

Reverse transcription-quantitative (RT-q)PCR. As previously described (21), total RNA was extracted from the HCC cells or tissues with RNAiso Plus (Takara Bio, Inc.). cDNA was synthesized using PrimeScript™ RT reagent Kit with gDNA Eraser (Takara Bio, Inc.). qPCR was performed using SYBR® Premix Ex Taq™ (Takara Bio, Inc.). The following thermocycling conditions were used: initial denaturation at 95°C for 30 sec followed by 40 cycles at 95°C for 5 sec and 60°C for 20 sec. Subsequently, the levels of gene expression were quantified using the 2^{-ΔΔC_q} method (24), and the values were normalized against GAPDH. The primer sequences are listed in Table S1.

Small interfering RNA (siRNA) synthesis, vector construction, and transfection. SPC25 shRNA, integrin subunit $\beta 4$ (*ITGB4*) small interfering (si)RNA and *ITGB4* cDNAs were synthesized by Bio-link-Gene Co., Ltd. The target sequences are listed in Table SII. Briefly, 3x10⁵ cells (Huh7 and HCCLM3) per well were seeded in 6-well plates the day before transfection. After 24 h, the lentiviruses were added to respective HCC cells with 1 ml of DMEM containing no FBS and 5 μ g/ml Polybrene (Sigma-Adrich; Merck KGaA). Twelve hours later, the medium was removed and replaced with fresh culture medium containing 10% FBS. Three days later, the cells were collected for subsequent culture. The efficiency of the transfections was confirmed using western blotting and RT-qPCR.

Microarray analysis. Total RNA was extracted from HCCLM3-shSPC25 and HCCLM3-shNC cells with RNAiso Plus (Takara Bio, Inc.). The Agilent SurePrint G3 Human Gene Expression v3 8x60K Microarray (Design ID: 072363) was used in this experiment, and data analysis of the 6 samples was conducted by OE Biotechnology Co., Ltd. (Shanghai, China). Total RNA was quantified by the NanoDrop ND-2000 (Thermo Fisher Scientific, Inc.) and the RNA integrity was assessed using Agilent Bioanalyzer 2100 (Agilent Technologies). The sample labeling, microarray hybridization and washing were performed based on the manufacturer's standard protocols. Briefly, total RNA was transcribed to double-strand cDNA, and then synthesized into cRNA and labeled with Cyanine-3-CTP. The labeled cRNAs were hybridized onto the microarray. After washing, the arrays were scanned by the Agilent Scanner G2505C (Agilent Technologies). Feature Extraction software (version 10.7.1.1; Agilent Technologies) was used to analyze array images to obtain raw data. Genespring (version 14.8, Agilent Technologies) was employed to finish the basic analysis with the raw data. Initially, the raw data were normalized with the quantile algorithm. The probes with at least 1 condition out of 2 conditions that had flags in 'Detected' were chosen for further data analysis. Differentially expressed genes were then identified through fold change as well as the P-value calculated with t-test. The threshold set for upregulated and downregulated genes was a fold change ≥ 1.0 and a P-value ≤ 0.05 . Afterwards, Gene Ontology (GO) analysis and Kyoto Encyclopedia of Genes and Genomes (KEGG) analysis were applied to determine the roles of these differentially expressed mRNAs. Finally, hierarchical clustering was performed to display the distinguishable gene expression patterns among the samples. We uploaded the raw data to the GEO database (GSE188881).

Wound healing assay. Cells (HCCLM3 and Huh7) were seeded at 80% confluency and cultured overnight. After the cells had been scratched using a 200- μ l pipette tip, they were cultured in FBS-free DMEM and the movement of the cells was measured every 12 h (up to 48 h) after scratching using a microscope (Olympus IX-71; Olympus Corp.), original magnification, x200. The wound distances were measured and calculated as a percentage of the distance at 0 h.

Transwell assay. Transwell assays were performed using Transwell chambers (Corning, Inc.) and Matrigel™ (Corning Life Sciences). For Transwell assays, the upper chamber coated with Matrigel was used for the invasion assays, whereas the migration assays were performed without Matrigel. The cells (HCCLM3 and Huh7) were seeded into the upper chamber and incubated for 36 h, and subsequently the chambers were stained with 0.1% crystal violet (Beyotime Institute of Biotechnology) for 10 min at 25°C. and counted in three different fields with a binocular optical microscope (Olympus Corp.) at original magnification, x200.

In vivo assay. As described in our previous studies (25,26), an *in vivo* assay was performed using nude mice (4-week-old male mice weighing approximately 20 g purchased from Charles River Laboratories, Inc.), which were randomly assigned to control and experimental groups (n=5). A total

of 6×10^6 cells (HCCLM3 and Huh7) were injected subcutaneously in the axilla of the nude mice. When the diameter of the subcutaneous tumor was 1-1.5 cm 4 weeks later, the subcutaneous tumors were obtained, which were used in an orthotopic model. The orthotopic model was established by orthotopic inoculation of tumor tissue (2x2x2 mm) into the livers of nude mice (n=5). When some mice developed ascites or cachexia after a subsequent 4-week period, the mice were sacrificed, and the tumor weights and volumes (largest diameter x perpendicular height²/2) were measured and analyzed. In this study, the largest diameter measured was 18 mm in for the HCCLM3 group, and 20 mm for the Huh7 group. The nude mice were euthanized via barbiturate overdose (sodium pentobarbital, 150 mg/kg), followed by exsanguination. General mouse health and well-being were monitored daily and no animals were withdrawn from the study. This research was conducted in strict accordance with the Care and Use of Laboratory Animals of the National Institutes of Health.

Western blot assay. As previously described (21), total protein was extracted using RIPA lysis buffer (Beyotime Institute of Biotechnology). Protein concentration was determined using a BCA assay (Beyotime Institute of Biotechnology). Total protein (30 μ g/lane) was separated using SDS-PAGE on a 10% gel (Beyotime Institute of Biotechnology) and transferred onto a PVDF membrane (MilliporeSigma). The membranes were blocked with 5% skimmed milk at room temperature for 1 h and incubated overnight at 4°C with diluted primary antibodies. Subsequently, the membranes were washed using TBS with 0.1% Tween-20 (TBST) three times and incubated with HRP-conjugated secondary antibodies for 1 h at room temperature. After being washed with TBST, the membranes were visualized using electrochemiluminescence (ECL) kit (Beyotime Institute of Biotechnology). B-actin was used as the loading control. The following antibodies were used: mouse monoclonal anti- β -actin (1:1,000; cat. no. AF0003; Beyotime Institute of Biotechnology), rabbit polyclonal anti-SPC25 (1:500; cat. no. ab121395; Abcam), rabbit monoclonal anti-ITGB4 [1:1,000; cat. no. 14803; Cell Signaling Technology, Inc. (CST)], rabbit monoclonal anti-PI3K (1:1,000; cat. no. 4257; CST), rabbit monoclonal anti-phospho-PI3K (1:1,000; cat. no. 17366; CST), rabbit monoclonal anti-AKT (1:1,000; cat. no. 4658; CST), rabbit monoclonal anti-phospho-AKT (1:1,000; cat. no. 4060; CST), rabbit monoclonal anti-FAK (1:1,000; cat. no. 13009; CST), rabbit monoclonal anti-phospho-FAK (1:1,000; cat. no. 8556; CST), rabbit monoclonal anti-MMP9 (1:1,000; cat. no. 13667; CST) and rabbit monoclonal anti-MMP13 (1:1,000; cat. no. 69926; CST), HRP-linked anti-rabbit secondary antibody (1:2,000; cat. no. 7074; CST), and HRP-linked anti-mouse secondary antibody (1:2,000; cat. no. 7076; CST). Three independent experiments were performed for each of the western blots.

Cell Counting Kit-8 (CCK-8) assay. The CCK-8 assay was performed using the CCK-8 assay kit of Dojindo Molecular Technologies, Inc. After 3,000 cells (HCCLM3 and Huh7) were seeded for 24, 48, and 72 h, 100 μ l reaction mixture (90 μ l DMEM and 10 μ l CCK-8 solution) was added and incubation was carried out for 2 h at 37°C. Finally, the absorbance was measured at 450 nm.

Statistical analysis. Statistical analyses were performed using SPSS Statistics 20.0 (IBM Corp.). Experimental data are presented as the mean \pm SD from three independent experiments performed in triplicate. The significant differences between groups were calculated by Student's t-test, Chi-square test or one-way ANOVA and Tukey post hoc test, as appropriate. The correlation analysis was performed using Spearman correlation analysis. Survival analysis was conducted using the Kaplan-Meier method, and comparisons were made using the log-rank test. Cox proportional hazards regression models were assessed using the relative prognostic significance of the variables for predicting overall survival (OS) and disease-free survival (DFS). P-values were two-tailed, and $P < 0.05$ was considered to indicate a statistically significant difference.

Results

Overexpression of SPC25 tissues is associated with poor prognosis in HCC. To study the role of SPC25 in HCC, the expression of SPC25 was first analyzed based on publicly available databases [The Cancer Genome Atlas (TCGA), International Cancer Genome Consortium (ICGC) and Gene Expression Omnibus (GEO)]. These analyses revealed that SPC25 is expressed at higher levels in HCC compared with that in normal liver tissues in the databases, TCGA [HCC (n=374) cf. normal (n=50) tissues, $P < 0.001$] (Fig. 1A), ICGC [HCC (n=240) cf. normal (n=202) tissues, $P < 0.001$] (Fig. 1B), GSE102079 [HCC (n=243) cf. normal (n=14) tissues, $P < 0.001$] (Fig. 1C) and GSE112790 [HCC (n=183) cf. normal (n=15) tissues, $P < 0.001$] (Fig. 1D). To validate these results, SPC25 expression was detected in 30 pairs of HCC and normal liver tissues using RT-qPCR, which confirmed that the expression of SPC25 in HCC tissues was indeed higher compared with the normal tissues (n=30, $P < 0.001$) (Fig. 1E).

To explore the association between SPC25 and HCC metastasis, the expression levels of SPC25 were detected in 141 pairs of HCC and normal liver tissues by IHC. This analysis revealed that SPC25 was expressed at a higher level in HCC tissues (n=141, $P < 0.001$) (Fig. 1F and G). Subsequently, the patients were divided into high and low expression groups, based on the median IOD of SPC25 expression.

Further analysis was conducted with the factors and the basic information related to HCC, which could objectively reflect the tumor burden and metastatic risk. The results revealed that thrombus, microvascular invasion (MVI), tumor number and encapsulation were markedly different when comparing the high and low expression groups (Table I), which strongly suggested that SPC25 may be involved in HCC malignancy, especially metastasis.

Kaplan-Meier analysis showed that SPC25 was associated with poor OS and DFS in HCC (Fig. 2A and B). The univariate and multivariate analyses revealed that SPC25 expression was an independent risk factor for OS [hazard ratio (HR), 1.864; 95% confidence interval (CI), 1.125-3.089; $P < 0.001$] and DFS (HR, 1.712; 95% CI, 1.097-2.672; $P = 0.018$) rates of patients with HCC (Table II). In order to validate these results, survival analysis was performed based on TCGA and ICGC data, which demonstrated that SPC25 was associated with poor OS rates (Fig. 2C and D). Therefore, it was possible to speculate that

Table I. Association between intratumor SPC25 and clinico-pathologic features (N=141) of the HCC patients.

Variable	SPC25		P-value
	Low	High	
Age (years)	52.61 \pm 11.4	54.12 \pm 10.3	0.316
Sex			0.379
Female	9	14	
Male	58	60	
Cirrhosis			0.180
No	11	19	
Yes	56	55	
Thrombus			0.002
No	65	59	
Yes	2	15	
Tumor size (cm)	6.34 \pm 3.36	8.57 \pm 4.12	0.091
MVI			0.042
No	49	42	
Yes	18	32	
Tumor number			0.039
Single	50	43	
Multiple	17	31	
Encapsulation			0.042
Yes	44	36	
No	23	38	

HCC, hepatocellular carcinoma; SPC25, spindle pole body component 25 homolog; MVI, microvascular invasion. $P < 0.05$ (Chi-square test or t-test) indicates a statistically significant difference and are indicated in bold print.

SPC25 overexpression was associated with the aggressiveness and poor prognosis of HCC.

SPC25 promotes invasion and migration of HCC cells in vitro and in vivo. Subsequently, western blotting was performed to assess the expression levels of SPC25 in the different liver cancer cell lines, and this analysis revealed that SPC25 was more highly expressed in HCCLM3 and Huh7 cells (Fig. 3A). SPC25 was then silenced in HCCLM3 and Huh7 cells using shRNAs, and its silencing was confirmed by western blotting and RT-qPCR (n=3, $P < 0.05$) (Fig. 3B and C). CCK-8 assay showed that SPC25 silencing led to a decrease in the proliferation of HCC cells (n=3, $P < 0.01$) (Fig. 3D). Wound healing assays were subsequently performed, and these experiments revealed that SPC25 silencing inhibited cell motility (n=3, $P < 0.05$) (Fig. 3E). Finally, Transwell assays consistently confirmed that SPC25 silencing inhibited the invasion and migration abilities of HCCLM3 and Huh7 cells (n=3, $P < 0.05$) (Fig. 3F). Taken together, the results obtained from these *in vitro* experiments suggested that SPC25 could facilitate HCC migration and invasion.

To explore the promotion of metastasis by SPC25 *in vivo*, transfected HCCLM3 and Huh7 cells were transplanted *in situ*

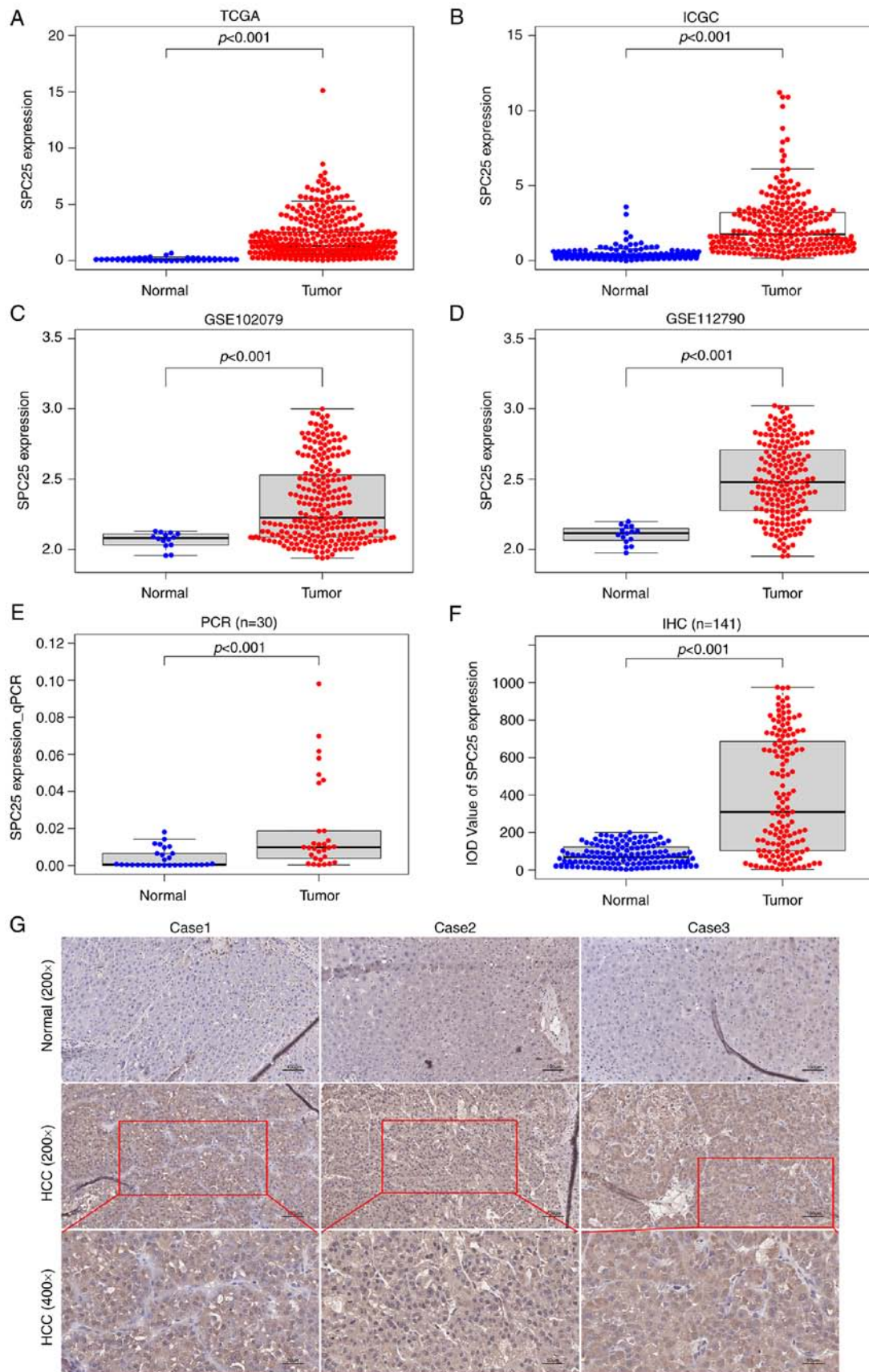


Figure 1. Differential expression analysis of SPC25 in HCC and normal liver tissues is shown. (A) TCGA [HCC (n=374) cf. normal (n=50) tissues, $P < 0.001$ (independent-samples t-test)]. (B) ICGC [HCC (n=240) cf. normal (n=202) tissues, $P < 0.001$ (independent-samples t-test)]. (C) GSE102079 [HCC (n=243) cf. normal (n=14) tissues, $P < 0.001$ (independent-samples t-test)]. (D) GSE112790 [HCC (n=183) cf. normal (n=15) tissues, $P < 0.001$ (independent-samples t-test)]. (E) The results from the RT-qPCR analysis is shown [n=30, $P < 0.001$ (matched samples t-test)]. (F) The results from the IHC analysis are shown [(n=141, $P < 0.001$) (matched samples t-test)]. (G) IHC staining indicated that SPC25 was expressed more highly in HCC tumor tissues compared with the expression in normal liver tissues. Original magnification, x200 (scale bars, 100 μm) and x400 (scale bars, 50 μm). SPC25, spindle pole body component 25 homolog; TCGA, The Cancer Genome Atlas; ICGC, International Cancer Genome Consortium; GEO, Gene Expression Omnibus; HCC, hepatocellular carcinoma.

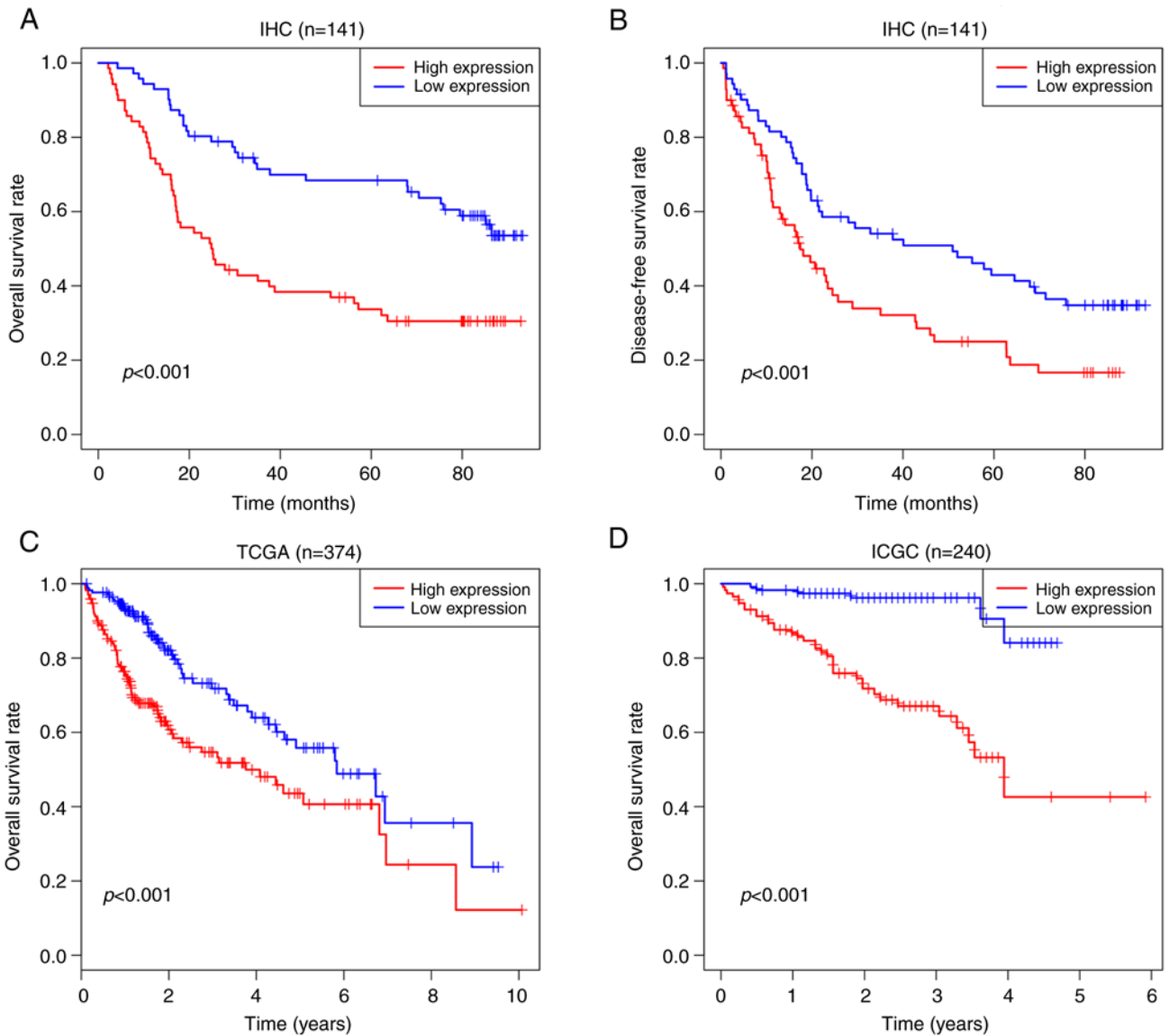


Figure 2. Kaplan-Meier analysis, showing that high expression of SPC25 is associated poor prognosis in HCC. (A) OS of patients at our center (n=141, $P < 0.001$). (B) DFS of patients at our center (n=141, $P < 0.001$). (C) OS of TCGA (n=374, $P < 0.001$). (D) OS of ICGC (n=240, $P < 0.001$). SPC25, spindle pole body component 25 homolog; HCC, hepatocellular carcinoma; OS, overall survival; DFS, disease-free survival; TCGA, The Cancer Genome Atlas; ICGC, International Cancer Genome Consortium.

into nude mice (n=5 each group). SPC25 silencing resulted in markedly reduced tumor sizes (n=5, $P < 0.05$) (Fig. 4A) and metastasis to the lungs (n=5, $P < 0.01$) (Fig. 4B). IHC staining with Ki-67 and E-cadherin antibodies suggested that SPC25 could promote tumor proliferation and metastasis (Fig. 4C). Therefore, these data support a role of SPC25 in promoting HCC metastasis *in vitro* and *in vivo*.

SPC25 upregulates the expression of genes associated with ECM-receptor interactions and focal adhesion pathways. To gain an improved understanding of the mechanism of SPC25 in promoting metastasis, Agilent cDNA microarray analysis was performed, and the gene expression levels of shSPC25 and shNC (negative control) in HCCLM3 cells were compared (GSE188881). A total of 1,091 differentially expressed genes (DEGs) were screened out, including 695 downregulated and 396 upregulated genes ($P < 0.05$, $\log_2 \text{FoldChange} \geq 1$) (Fig. 5A).

Subsequently, Gene Ontology (GO) and Kyoto Encyclopedia of Genes and Genomes (KEGG) enrichment analysis was performed. The results obtained showed that SPC25 silencing mainly influenced the functions ‘extracellular region cellular component’, ‘small molecule binding molecular function’, ‘extracellular matrix organization biological process’ (Fig. 5B) and ‘ECM-receptor interactions’ (Fig. 5C). The ECM-receptor interactions included numerous genes that promote metastasis and cell motility, a finding that was in keeping with the metastasis-promoting role of SPC25. Subsequently, RT-qPCR was used to confirm the genes identified by microarray analysis in SPC25-silenced cells (n=3, $P < 0.05$) (Fig. 5D). The results obtained showed that SPC25 could affect the expression of metastasis-associated genes.

SPC25-mediated promotion of metastasis is mediated by ITGB4. Among the DEGs, ITGB4 is an integrin-encoding

Table II. Univariate and multivariate analysis of factors associated with overall survival and disease-free survival of the HCC patients.

Factor	Overall survival				Disease-free survival			
	Univariate P-value	Multivariate			Univariate P-value	Multivariate		
		HR	95% CI	P-value		HR	95% CI	P-value
Age (years) (≤ 50 vs. >50)	0.707			NA	0.495			NA
Sex (female vs. male)	0.676			NA	0.877			NA
Cirrhosis (no vs. yes)	0.489			NA	0.447			NA
Tumor size (cm) (≤ 5 vs. >5)	0.002	1.541	0.882-2.691	NS	0.002	1.743	1.089-2.791	0.021
Tumor number (single vs. multiple)	0.918			NA	0.675			NA
MVI (no vs. yes)	0.002	2.296	1.432-3.680	0.001	0.002	1.347	0.857-2.119	NS
Thrombus (no vs. yes)	<0.001	2.283	1.244-4.187	0.008	<0.001	2.922	1.527-5.558	0.001
Encapsulation (no vs. yes)	0.377			NA	0.300			NA
SPC25 (high vs. low)	<0.001	1.864	1.125-3.089	0.016	<0.001	1.712	1.097-2.672	0.018

HCC, hepatocellular carcinoma; SPC25, spindle pole body component 25 homolog; MVI, microvascular invasion; NA, not applicable; NS, not significant; HR, hazard ratio; CI, confidence interval. $P < 0.05$ indicates a statistically significant difference and significant P-values are indicated in bold print.

gene, and laminin subunit $\alpha 1$ (LAMA1), laminin subunit $\alpha 3$ (LAMA3), laminin subunit $\alpha 4$ (LAMA4) and laminin subunit $\gamma 3$ (LAMC3) are laminin-coding genes that lie upstream of the integrin pathway. Therefore, our conjecture was that SPC25 may control ECM-integrin interactions to regulate the integrin pathway. The associations among SPC25 and ITGB4, LAMA1, LAMA3, LAMA4 and LAMC3 were analyzed based on the HCC data of TCGA, which revealed that ITGB4 and SPC25 had the strongest positive correlation ($n=369$; $\rho_{\text{spearman}}=0.34$; 95% CI: 0.25-0.43; $P < 0.001$) (Fig. 6A and Fig. S1). Subsequently, the correlation between ITGB4 and SPC25 was analyzed based on the data of HCC tissues by RT-qPCR, which revealed that ITGB4 and SPC25 were positively correlated ($n=30$; $\rho_{\text{spearman}}=0.451$; 95% CI: 0.16-0.64; $P < 0.01$) (Fig. 6B). Finally, the decrease in ITGB4 in response to SPC25 knockdown was confirmed via western blot analysis ($n=3$, $P < 0.01$) (Fig. 6C). Taken together, these results indicated that ITGB4 may be a downstream target of SPC25.

Since the results obtained suggest a role for SPC25 in promoting metastasis, the role of ITGB4 in the transmission of HCC metastatic potential was subsequently explored. Silencing of ITGB4 caused a significant reduction in the invasion and migration abilities of HCCLM3 and Huh7 cells *in vitro* ($n=3$, $P < 0.01$) (Fig. 6D). The findings revealed that ITGB4 and SPC25 have a similar role in promoting HCC metastasis. Subsequently, rescue experiments were performed to explore whether SPC25 could promote HCC metastasis via ITGB4. The results obtained showed that ectopic overexpression of ITGB4 with simultaneous silencing of SPC25 partially mitigated the reduction in cell invasion and migration capability caused by SPC25 silencing ($n=3$, $P < 0.05$) (Fig. 6E). Hence, these results suggest that ITGB4 is the main downstream mediator of SPC25-induced metastatic activity.

SPC25 activates the FAK/PI3K/AKT signaling pathway through ITGB4. A previous study has shown that integrin-laminin binding increases FAK phosphorylation, which induces activation of the PI3K/AKT signaling pathway to promote tumor metastasis (10). In the present study, the results obtained showed that neither SPC25 nor ITGB4 silencing exerted any effect on the total protein levels of FAK, PI3K and AKT, whereas their silencing did markedly reduce the levels of phosphorylated (p)-FAK, p-PI3K and p-AKT ($n=3$, $P < 0.05$) (Fig. 7A) and the ratios of phosphorylated vs. total protein (PI3K, FAK and AKT) (Fig. S2A). Subsequently, rescue experiments were performed, and ITGB4 overexpression was observed to reverse the decrease in expression of p-FAK, p-PI3K and p-AKT levels induced by SPC25 silencing ($n=3$, $P < 0.05$) (Fig. 7B) and the ratios of phosphorylated vs. total protein (PI3K, FAK and AKT) (Fig. S2B). Furthermore, SPC25 silencing was also found to decrease the expression of MMP9 and MMP13 ($n=3$, $P < 0.05$) (Fig. 7C and D), which are proteins involved in the FAK/PI3K/AKT signaling pathway. Taken together, these findings suggest that SPC25 could promote HCC metastasis, mainly through regulating ITGB4 to activate the FAK/PI3K/AKT signaling pathway.

Discussion

The present study has mainly focused on the role of spindle pole body component 25 homolog (SPC25) in promoting metastasis in hepatocellular carcinoma (HCC), and in the underlying mechanism. Previous studies have shown that SPC25 is able to promote HCC proliferation, and that it was found to be a prognostic indicator of poor survival in patients with HCC (18-20). However, these studies were mainly based on bioinformatics analysis, and relevant experimental studies have found only an *in vitro* phenomenon. There are no in-depth and reliable experimental studies on the specific

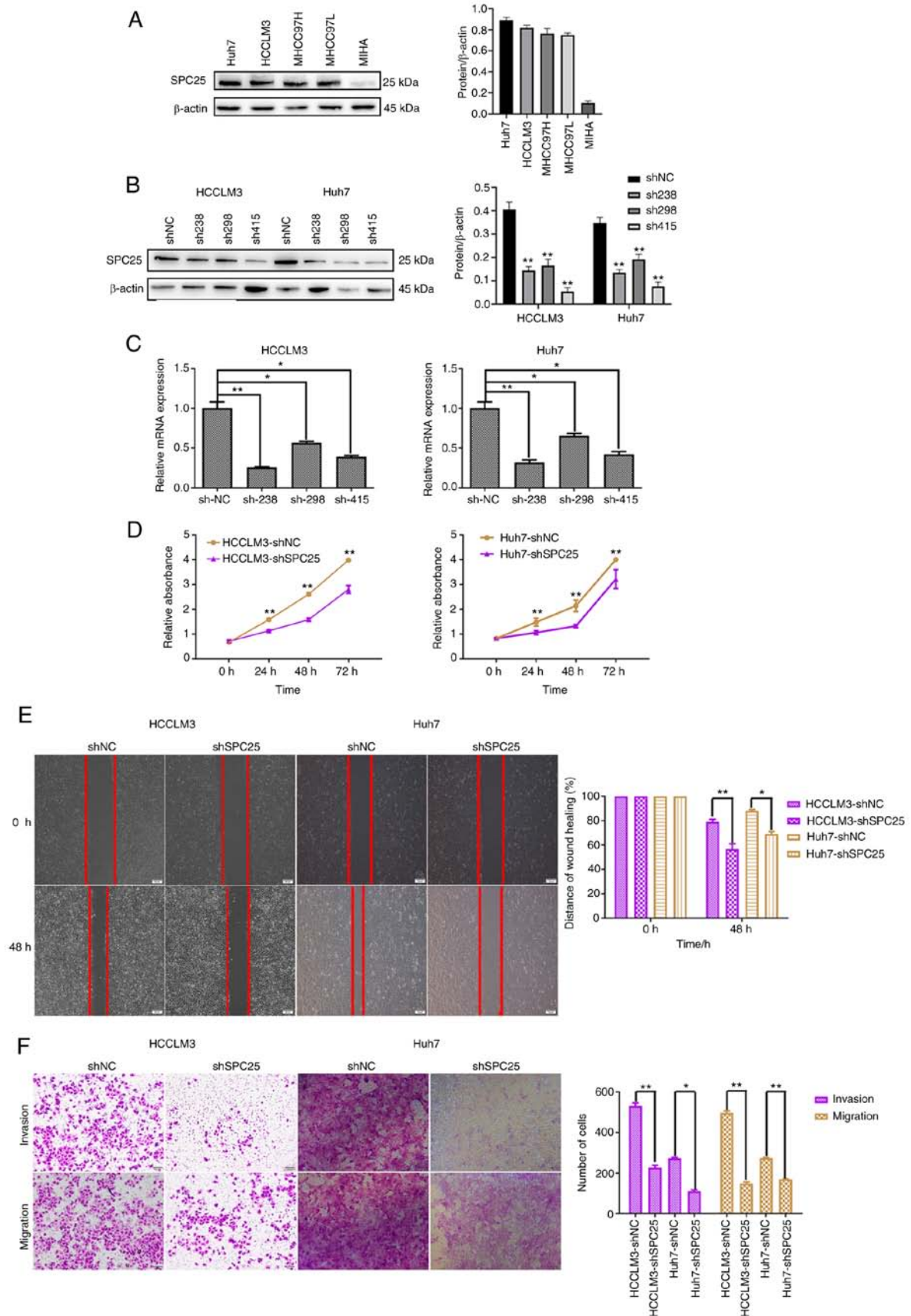


Figure 3. SPC25 promotes HCC migration *in vitro*. (A) Western blot analysis revealed the levels of SPC25 protein expression in liver cancer cell lines. (B and C) Western blotting and RT-qPCR were used to confirm the silencing of SPC25 in the HCC cell lines ($P < 0.05$ and $^{**}P < 0.01$, one-way ANOVA, compared with the shNC). (D) CCK-8 assay indicated that SPC25 silencing reduced the proliferation of Huh7 and HCCLM3 cells ($^{**}P < 0.001$, independent-samples t-test, compared with the shNC group). (E) Wound-healing assay was used to show that SPC25 silencing reduced the migration of Huh7 and HCCLM3 cells. Original magnification, $\times 200$. Scale bars, $50 \mu\text{m}$ ($P < 0.05$ and $^{**}P < 0.01$, independent-samples t-test, compared to the shNC group). (F) Transwell assay, indicating that SPC25 silencing reduced the invasion and migration of Huh7 and HCCLM3 cells ($P < 0.05$, $^{**}P < 0.01$, independent-samples t-test, compared to the shNC group). Original magnification, $\times 200$. Scale bars, $100 \mu\text{m}$. SPC25, spindle pole body component 25 homolog; HCC, hepatocellular carcinoma.

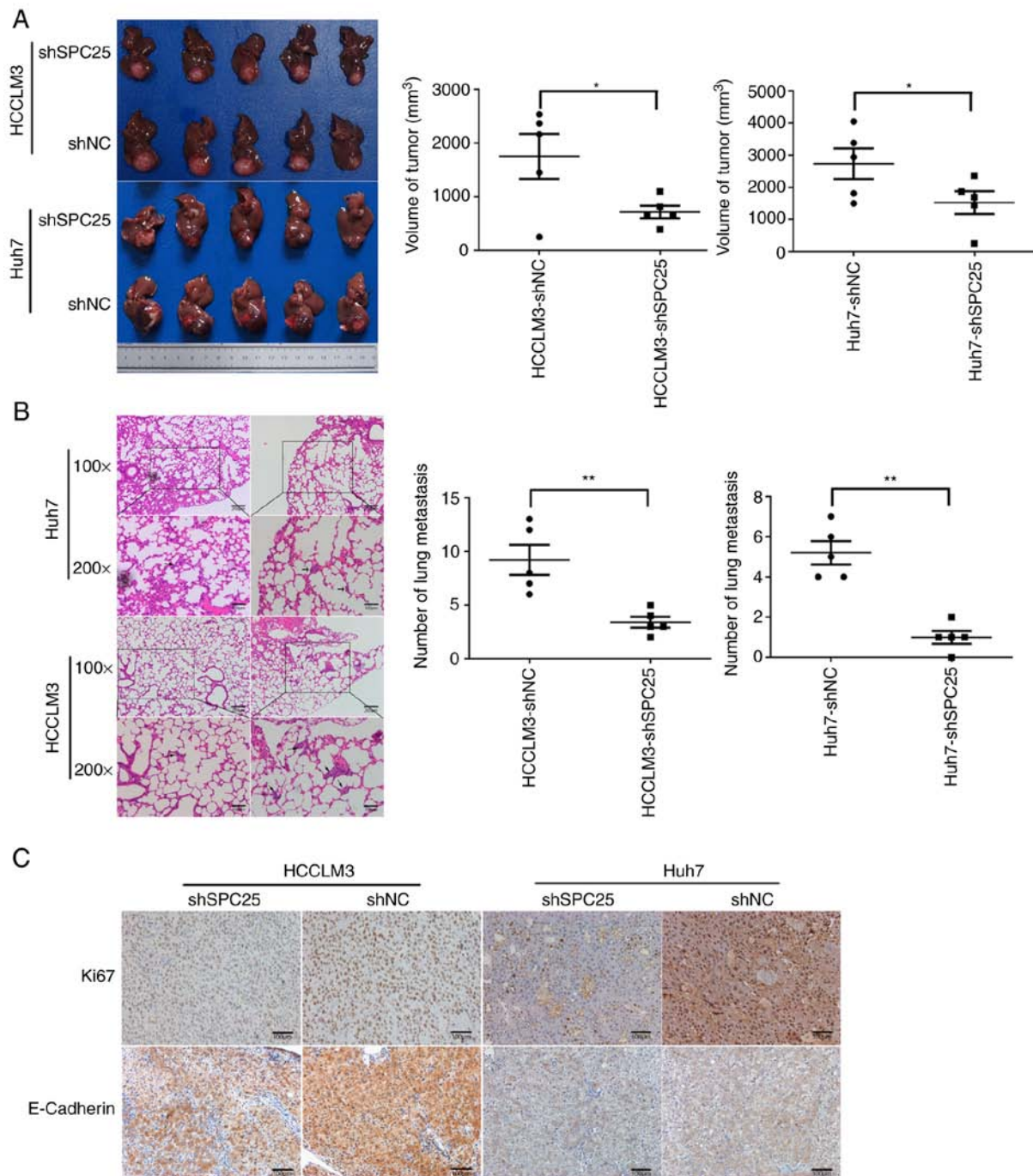


Figure 4. SPC25 promotes HCC metastasis *in vivo*. (A) An *in vivo* assay was performed to show that SPC25 silencing could reduce the growth of Huh7 and HCCLM3 cells (tumors in the liver tissues) ($P < 0.05$, independent-samples t-test, compared to the shNC group). (B) SPC25 silencing reduced the lung metastasis of Huh7 and HCCLM3 cells ($P < 0.01$, independent-samples t-test, compared to the shNC group). (C) IHC staining indicated that SPC25 silencing could reduce the expression of Ki67 and E-cadherin *in vivo*. Original magnification, x200. Scale bars, 100 μ m. SPC25, spindle pole body component 25 homolog; HCC, hepatocellular carcinoma.

roles and mechanisms of SPC25 in HCC. In the present study, the expression of SPC25 was first examined in specimens from 141 patients with HCC and survival analyses were performed to verify the results from the public database. We firstly detected the changes of genes and signaling pathways in HCC cells (HCCLM3) induced by SPC25 knockdown by Agilent cDNA microarray analysis and uploaded the relevant data to the GEO database (GSE188881). Based on the results, we identified the main pathway of SPC25 regulating the invasion and metastasis of HCC cells and was verified by rescue

experiments. In conclusion, we firstly examined the role and mechanism of SPC25 in regulating the invasion and metastasis of HCC cells in a systematic and in-depth experimental study.

In the present study, SPC25 expression was examined in HCC tissues, and microarray analysis was performed to clarify the mechanism. SPC25 was found to be expressed highly in HCC tissues, and this high level of expression was associated with thrombus, microvascular invasion (MVI), tumor number and encapsulation, suggesting that SPC25 may be a predictor for HCC prognosis and metastasis. Subsequently, further

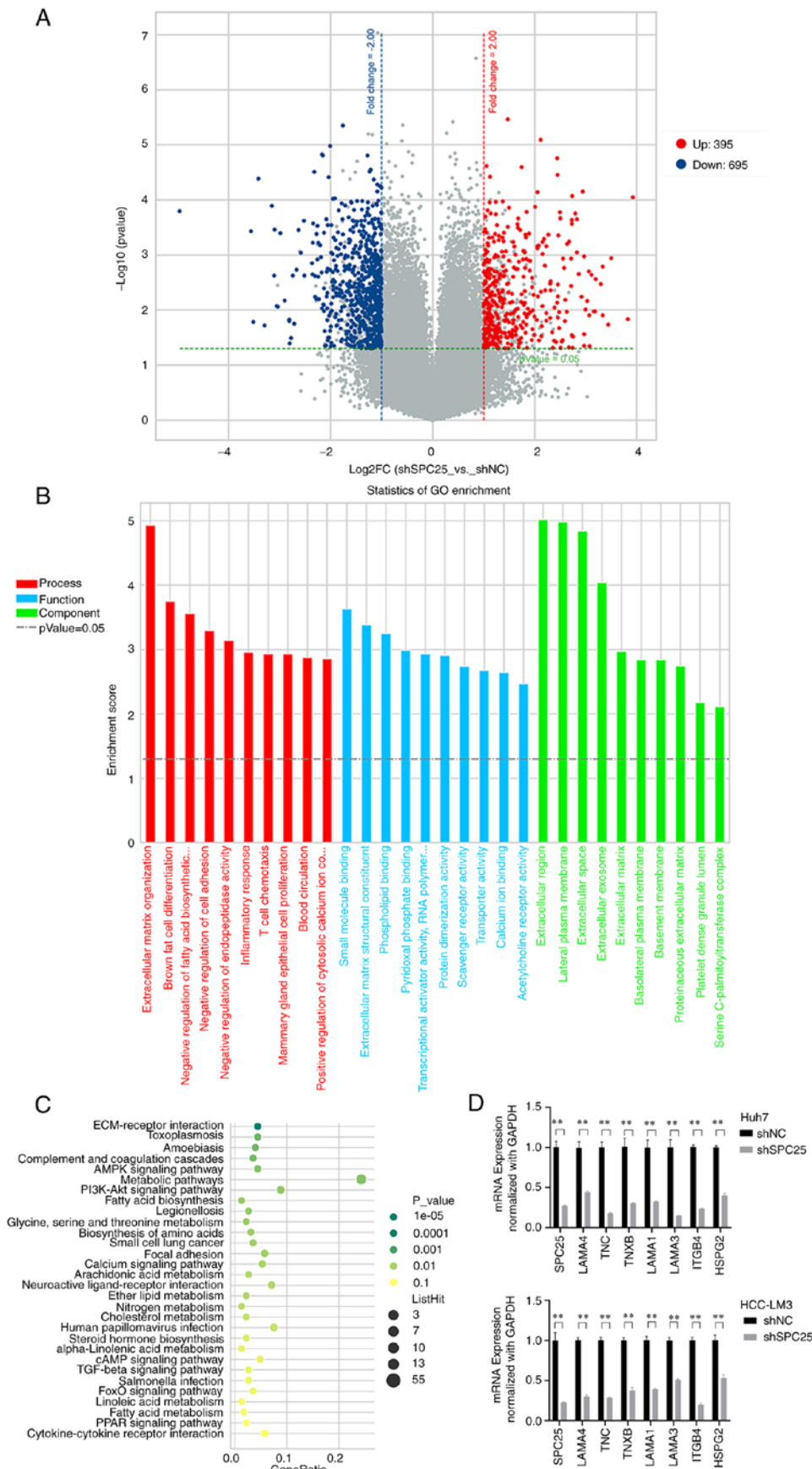


Figure 5. SPC25 upregulates the expression of genes associated with ECM-receptor interactions and focal adhesion pathways. (A) The volcano map of DEGs (HCLM3 silencing vs. control). (B) GO analysis showed that SPC25 exerts an influence on ECM-associated biological processes. (C) KEGG analysis, also revealing that SPC25 silencing exerts important effects on ECM-receptor interactions. (D) The genes associated with ECM-receptor interactions and focal adhesion were screened by microarray analysis, and subsequently confirmed by RT-qPCR (**P<0.01, independent-samples t-test, compared with the shNC group). SPC25, spindle pole body component 25 homolog; DEG, differentially expressed gene; GO, Gene Ontology; KEGG, Kyoto Encyclopedia of Genes and Genomes; ECM, extracellular matrix.

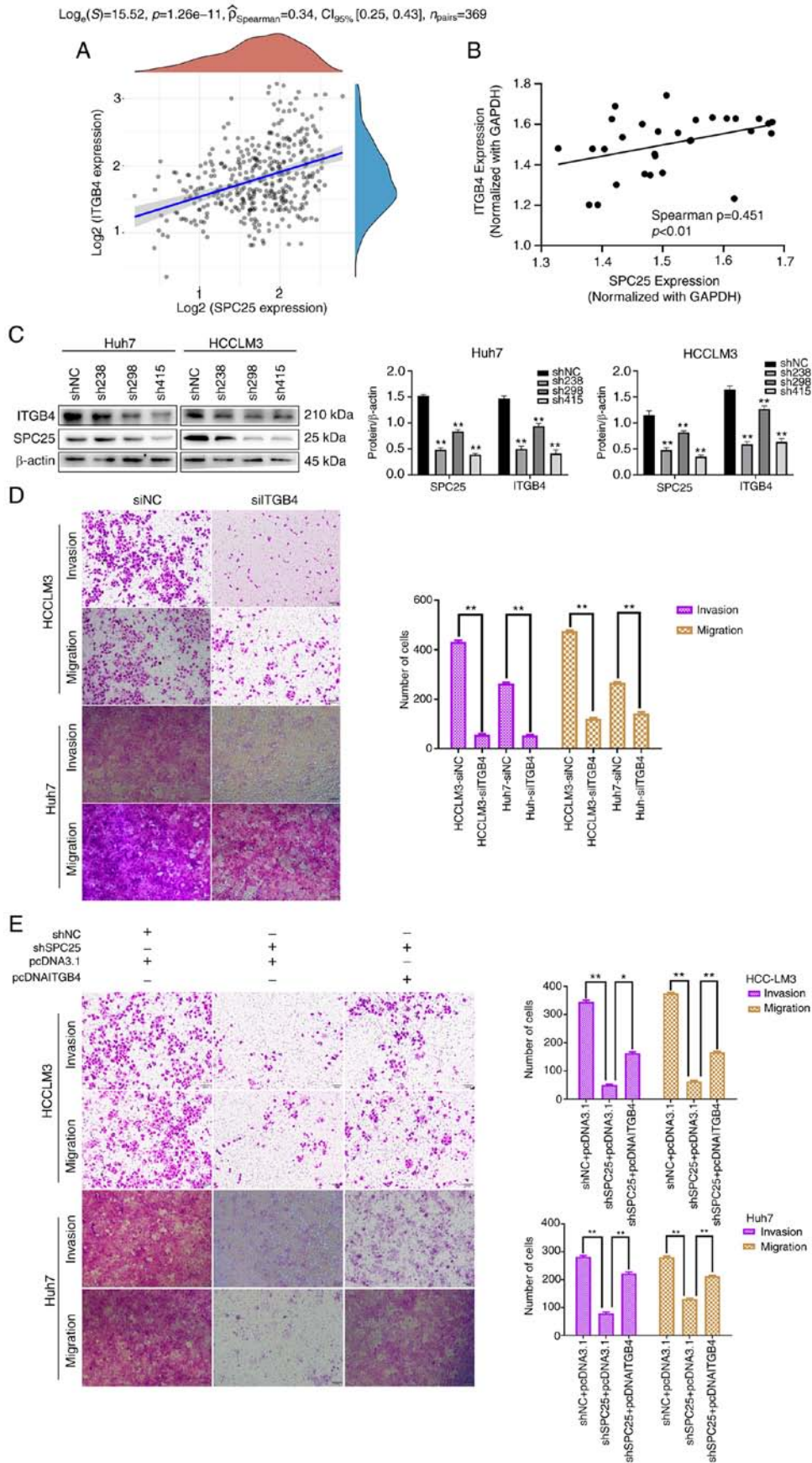


Figure 6. Promotion of metastasis by SPC25 is mediated by ITGB4. (A) Correlation analysis of SPC25 and ITGB4 based on TCGA data is shown. (B) Correlation analysis of SPC25 and ITGB4 by RT-qPCR is shown. (C) Western blot analysis showed that alterations in the level of ITGB4 were accompanied by changes in the level of SPC25 ($^{**}P < 0.01$, one-way ANOVA, compared with the shNC group). (D) Transwell assay, showing that ITGB4 silencing reduced the invasion and migration of Huh7 and HCCLM3 cells ($^{**}P < 0.01$, independent-samples t-test). (E) A rescue experiment with Transwell assays was performed in Huh7 and HCCLM3 cells co-transfected with shNC or shSPC25 and pcDNA3.1 or pcITGB4 ($^{*}P < 0.05$ and $^{**}P < 0.01$, one-way ANOVA). Original magnification, x200. Scale bars, 100 μm . 001. SPC25, spindle pole body component 25 homolog; ITGB4, integrin subunit $\beta 4$; TCGA, The Cancer Genome Atlas.

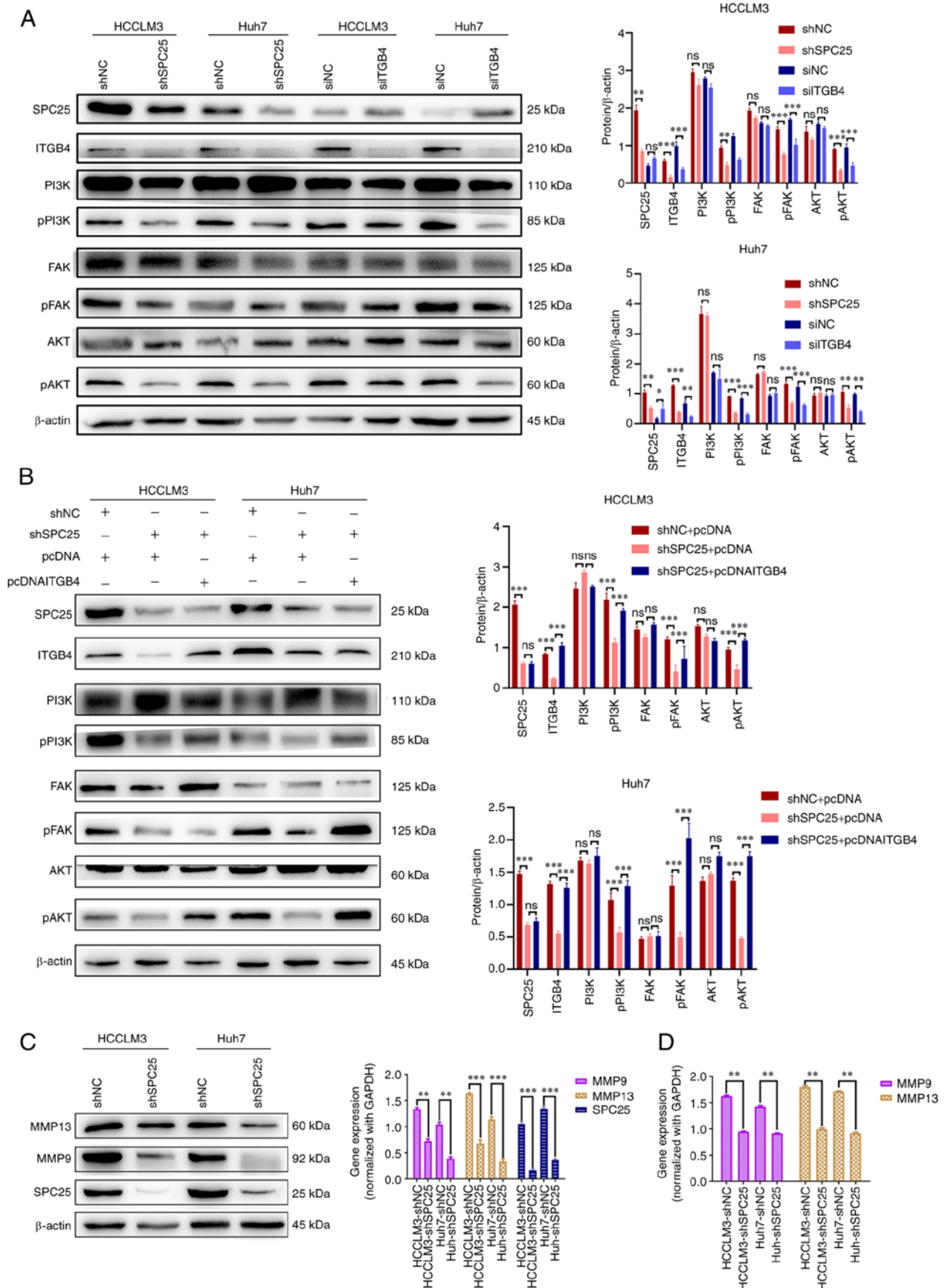


Figure 7. SPC25 activates the FAK/PI3K/AKT signaling pathway through ITGB4. (A) Western blot analysis revealed the changed levels in phosphorylated (p) FAK, pPI3K and pAKT after SPC25 or ITGB4 silencing in Huh7 and HCCLM3 cells ($P < 0.05$, $**P < 0.01$, $***P < 0.001$; ns, not significant, independent-samples t-test). (B) Western blot analysis, revealing the results of the rescue experiment on proteins associated with the FAK/PI3K/AKT signaling pathway ($***P < 0.001$; ns, not significant, one-way ANOVA). (C and D) The altered levels of MMP9 and MMP13 in Huh7 and HCCLM3 after SPC25 silencing are shown [(C) Results of western blot, (D) Results of RT-qPCR ($**P < 0.01$, $***P < 0.001$, independent-samples t-test)]. SPC25, spindle pole body component 25 homolog; FAK, focal adhesion kinase; ITGB4, integrin subunit $\beta 4$; p, phosphorylated; MMP, matrix metalloproteinase; PI3K, phosphoinositide 3-kinase.

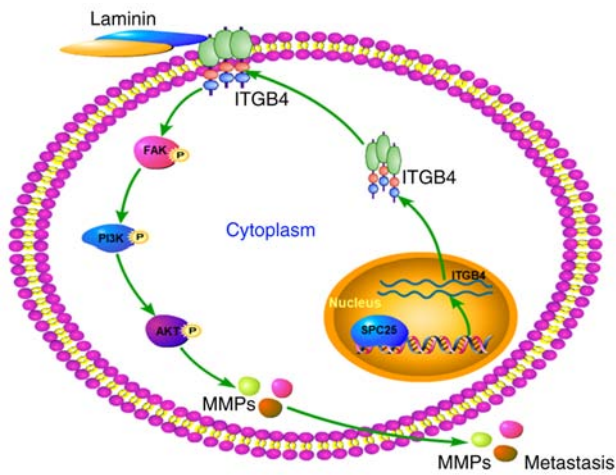


Figure 8. Model of the signaling pathway involved in the promotion of HCC metastasis by SPC25. In the nucleus, SPC25 facilitates ITGB4 transcription. Subsequently in the cytoplasm, ITGB4 binds to laminin on the cell membrane and activates the FAK/PI3K/AKT signaling pathway, thereby promoting HCC metastasis. SPC25, spindle pole body component 25 homolog; HCC, hepatocellular carcinoma; ITGB4, integrin subunit β 4; FAK, focal adhesion kinase; PI3K, phosphoinositide 3-kinase.

experiments revealed that SPC25 could accelerate HCC metastasis both *in vivo* and *in vitro*.

The present study also demonstrated that SPC25 accelerated HCC metastasis by regulating a number of genes that are associated with extracellular matrix (ECM)-integrin interactions. A previously published study revealed that integrin imbalances resulting from genomic variation or expression disorder are associated with tumorigenesis (27). For example, ITGB4 was shown to be associated with the progression of NSCLC, pancreatic cancer, colon cancer, prostate cancer and other types of cancer (28-31). In particular, ITGB4 expression is often found at the forefront of cancer cell invasion (32,33). In the present study, it was found that ITGB4 expression decreased with SPC25 silencing. Moreover, ITGB4 exerted the same role as SPC25 in terms of promoting HCC metastasis. In addition, it was found that SPC25 is closely associated with the expression of ITGB4 in HCC tissues, and that upregulation of ITGB4 partly alleviated the reduced cell migration ability caused by downregulated expression of the SPC25 gene. Collectively, these results provided sufficient evidence for the hypothesis that ITGB4 may be a target gene of SPC25.

In the present study, it has also been shown that SPC25 promotes HCC metastasis mainly through activation of the FAK/PI3K/AKT signaling pathway. ECM proteins locally adhere to integrin elements on the cell membrane, forming the basic adhesive molecule known as a hemidesmosome (34,35). Upon ligation, FAK becomes phosphorylated to activate the PI3K/AKT signaling pathway, a phenomenon that has also been reported in HCC and gastric cancer (12,36). In the present study, the results showed that silencing both SPC25 and ITGB4 reduced the activation of FAK, PI3K and AKT. Furthermore, the upregulation of ITGB4 inhibited the inactivation induced by SPC25 silencing. Activated signaling pathways often occur in many different tumor types, and the regulatory networks among them are particularly complex. The present study demonstrated that ITGB4 could induce the phosphorylation of FAK, and the PI3K/AKT signaling pathway was identified as being affected by SPC25. It has also

been shown that the activated FAK/PI3K/AKT signaling pathway induced by SPC25 was regulated via ECM-integrin interactions.

Genomic instability fulfills an important role in tumor metastasis (37,38), and metastasis is the leading cause of cancer-associated deaths (5). SPC25, as a gene associated with genomic instability, has an important role in promoting HCC metastasis. The results based on clinical samples in the present study showed that SPC25 is associated with thrombus, MVI, tumor number and encapsulation, which are indicators either of tumor metastasis or a high propensity for metastasis. In analyzing the underlying mechanism, it was found that SPC25 could activate the FAK/PI3K/AKT signaling pathway and regulate ECM-integrin interactions to promote metastasis in HCC. Based on these findings, it is possible to conclude that SPC25 is able to regulate the invasion and metastasis of HCC cells, and promote metastasis in patients with HCC. Considering all the results obtained and this discussion thus far, we consider that targeting SPC25 as a means of therapeutic intervention may be a viable strategy for reducing the invasive ability of HCC cells, thereby improving the survival time of the patients.

In conclusion, the present study suggests a role for SPC25 as a prognostic indicator, as SPC25 was shown to be able to promote metastasis in HCC. The results obtained have demonstrated that SPC25 is able to promote metastasis through the ITGB4-mediated FAK/PI3K/AKT signaling pathway (Fig. 8). This study has enabled us to recognize the importance of SPC25 and its role in the invasion and migration of HCC cells and, consequently, its potential prognostic and therapeutic value.

Acknowledgements

Not applicable.

Funding

This study was supported by the Joint Construction Project of Medical Science and Technology of Henan Province (grant no. LHGJ20190041).

Availability of data and materials

The datasets used and/or analyzed during the current study are available from the corresponding author on reasonable request.

Authors' contributions

WKS and YFZ conceived and designed the study. WKS and QLS analyzed the data and wrote the paper. WKS, QLS and YFZ were all involved in preparing the manuscript of the study. All authors read and approved the manuscript, and agree to be accountable for all aspects of the research in ensuring that the accuracy or integrity of any part of the work in particular the data are appropriately investigated and resolved.

Ethics approval and consent to participate

This study was approved by the Institutional Review Board of the First Affiliated Hospital of Zhengzhou University before specimen collection and animal tests (approval no. 2019-KY-21). All patients provided signed informed

consent, and the collection of clinical samples was conducted in accordance with the Declaration of Helsinki. The animal tests in this study complied with the ethical guidelines of the Laboratory Animal Care International Council for Science (ICLAS) and the NC3Rs ARRIVE Guidelines.

Patient consent for publication

Not applicable.

Competing interests

The authors declare that they have no competing interests.

References

- Hindson J: Lenvatinib plus EGFR inhibition for liver cancer. *Nat Rev Gastroenterol Hepatol* 18: 675, 2021.
- Villanueva A: Hepatocellular carcinoma. *N Engl J Med* 380: 1450-1462, 2019.
- Llovet JM, Ricci S, Mazzaferro V, Hilgard P, Gane E, Blanc JF, de Oliveira AC, Santoro A, Raoul JL, Forner A, *et al*: SHARP investigators study group: Sorafenib in advanced hepatocellular carcinoma. *N Engl J Med* 359: 378-390, 2008.
- Kudo M, Finn RS, Qin S, Han KH, Ikeda K, Piscaglia F, Baron A, Park JW, Han G, Jassem J, *et al*: Lenvatinib versus sorafenib in first-line treatment of patients with unresectable hepatocellular carcinoma: A randomised phase 3 non-inferiority trial. *Lancet* 391: 1163-1173, 2018.
- Bruix J, da Fonseca LG and Reig M: Insights into the success and failure of systemic therapy for hepatocellular carcinoma. *Nat Rev Gastroenterol Hepatol* 16: 617-630, 2019.
- Quail DF and Joyce JA: Microenvironmental regulation of tumor progression and metastasis. *Nat Med* 19: 1423-1437, 2013.
- Holle AW, Young JL and Spatz JP: In vitro cancer cell-ECM interactions inform in vivo cancer treatment. *Adv Drug Deliv Rev* 97: 270-279, 2016.
- Mitra SK and Schlaepfer DD: Integrin regulated FAK-Src signaling in normal and cancer cells. *Curr Opin Cell Biol* 18: 516-523, 2006.
- Kim SH, Turnbull J and Guimond S: Extracellular matrix and cell signalling: The dynamic cooperation of integrin, proteoglycan and growth factor receptor. *J Endocrinol* 209: 139-151, 2011.
- Liang Y, Chen X, Wu Y, Li J, Zhang S, Wang K, Guan X, Yang K and Bai Y: LncRNA CASC9 promotes esophageal squamous cell carcinoma metastasis through upregulating LAMC2 expression by interacting with the CREB-binding protein. *Cell Death Differ* 25: 1980-1995, 2018.
- Tai YL, Chu PY, Lai IR, Wang MY, Tseng HY, Guan JL, Liou JY and Shen TL: An EGFR/Src-dependent $\beta 4$ integrin/FAK complex contributes to malignancy of breast cancer. *Sci Rep* 5: 16408, 2015.
- Leng C, Zhang ZG, Chen WX, Luo HP, Song J, Dong W, Zhu XR, Chen XP, Liang HF and Zhang BX: An integrin $\beta 4$ -EGFR unit promotes hepatocellular carcinoma lung metastases by enhancing anchorage independence through activation of FAK-AKT pathway. *Cancer Lett* 376: 188-196, 2016.
- Sun SC, Lee SE, Xu YN and Kim NH: Perturbation of Spc25 expression affects meiotic spindle organization, chromosome alignment and spindle assembly checkpoint in mouse oocytes. *Cell Cycle* 9: 4552-4559, 2010.
- Aguilera A and Garcia-Muse T: Causes of genome instability. *Annu Rev Genet* 47: 1-32, 2013.
- Chen J, Chen H, Yang H and Dai H: SPC25 upregulation increases cancer stem cell properties in non-small cell lung adenocarcinoma cells and independently predicts poor survival. *Biomed Pharmacother* 100: 233-239, 2018.
- Wang Q, Zhu Y, Li Z, Bu Q, Sun T, Wang H, Sun H and Cao X: Up-regulation of SPC25 promotes breast cancer. *Aging (Albany NY)* 11: 5689-5704, 2019.
- Cui F, Tang H, Tan J and Hu J: Spindle pole body component 25 regulates stemness of prostate cancer cells. *Aging (Albany NY)* 10: 3273-3282, 2018.
- Yang X, Sun H, Song Y, Yang L and Liu H: Diagnostic and prognostic values of upregulated SPC25 in patients with hepatocellular carcinoma. *PeerJ* 8: e9535, 2020.
- Zhang B, Zhou Q, Xie Q, Lin X, Miao W, Wei Z, Zheng T, Pang Z, Liu H and Chen X: SPC25 overexpression promotes tumor proliferation and is prognostic of poor survival in hepatocellular carcinoma. *Aging (Albany NY)* 13: 2803-2821, 2021.
- Chen F, Zhang K, Huang Y, Luo F, Hu K and Cai Q: SPC25 may promote proliferation and metastasis of hepatocellular carcinoma via p53. *FEBS Open Bio* 10: 1261-1275, 2020.
- Shi WK, Zhu XD, Wang CH, Zhang YY, Cai H, Li XL, Cao MQ, Zhang SZ, Li KS and Sun HC: PFKFB3 blockade inhibits hepatocellular carcinoma growth by impairing DNA repair through AKT. *Cell Death Dis* 9: 428, 2018.
- Chiyonobu N, Shimada S, Akiyama Y, Mogushi K, Itoh K, Akahoshi K, Matsumura S, Ogawa K, Ono H, Mitsunori Y, *et al*: Fatty Acid Binding Protein 4 (FABP4) overexpression in intratumoral hepatic stellate cells within hepatocellular carcinoma with metabolic risk factors. *Am J Pathol* 188: 1213-1224, 2018.
- Shimada S, Mogushi K, Akiyama Y, Furuyama T, Watanabe S, Ogura T, Ogawa K, Ono H, Mitsunori Y, Ban D, *et al*: Comprehensive molecular and immunological characterization of hepatocellular carcinoma. *EBioMedicine* 40: 457-470, 2019.
- Livak KJ and Schmittgen TD: Analysis of relative gene expression data using real-time quantitative PCR and the 2⁻(-Delta Delta C(T)) method. *Methods* 25: 402-408, 2001.
- Sun FX, Tang ZY, Lui KD, Ye SL, Xue Q, Gao DM and Ma ZC: Establishment of a metastatic model of human hepatocellular carcinoma in nude mice via orthotopic implantation of histologically intact tissues. *Int J Cancer* 66: 239-243, 1996.
- Wang CH, Zhu XD, Ma DN, Sun HC, Gao DM, Zhang N, Qin CD, Zhang YY, Ye BG, Cai H, *et al*: Flot2 promotes tumor growth and metastasis through modulating cell cycle and inducing epithelial-mesenchymal transition of hepatocellular carcinoma. *Am J Cancer Res* 7: 1068-1083, 2017.
- Lee JS and Thorgeirsson SS: Functional and genomic implications of global gene expression profiles in cell lines from human hepatocellular cancer. *Hepatology* 35: 1134-1143, 2002.
- Li M, Jiang X, Wang G, Zhai C, Liu Y, Li H, Zhang Y, Yu W and Zhao Z: ITGB4 is a novel prognostic factor in colon cancer. *J Cancer* 10: 5223-5233, 2019.
- Wu P, Wang Y, Wu Y, Jia Z, Song Y and Liang N: Expression and prognostic analyses of *ITGA11*, *ITGB4* and *ITGB8* in human non-small cell lung cancer. *PeerJ* 7: e8299, 2019.
- Wilkinson EJ, Woodworth AM, Parker M, Phillips JL, Malley RC, Dickinson JL and Holloway AF: Epigenetic regulation of the ITGB4 gene in prostate cancer. *Exp Cell Res* 392: 112055, 2020.
- Zhuang H, Zhou Z, Ma Z, Li Z, Liu C, Huang S, Zhang C and Hou B: Characterization of the prognostic and oncologic values of ITGB superfamily members in pancreatic cancer. *J Cell Mol Med* 24: 13481-13493, 2020.
- Sung JS, Kang CW, Kang S, Jang Y, Chae YC, Kim BG and Cho NH: ITGB4-mediated metabolic reprogramming of cancer-associated fibroblasts. *Oncogene* 39: 664-676, 2020.
- Li XL, Liu L, Li DD, He YP, Guo LH, Sun LP, Liu LN, Xu HX and Zhang XP: Integrin $\beta 4$ promotes cell invasion and epithelial-mesenchymal transition through the modulation of Slug expression in hepatocellular carcinoma. *Sci Rep* 7: 40464, 2017.
- Wang W, Zuidema A, Te Molder L, Nahidiazar L, Hoekman L, Schmidt T, Coppola S and Sonnenberg A: Hemidesmosomes modulate force generation via focal adhesions. *J Cell Biol* 219: e201904137, 2020.
- Walko G, Castañón MJ and Wiche G: Molecular architecture and function of the hemidesmosome. *Cell Tissue Res* 360: 363-378, 2015.
- Xu L, Hou Y, Tu G, Chen Y, Du YE, Zhang H, Wen S, Tang X, Yin J, Lang L, *et al*: Nuclear Drosha enhances cell invasion via an EGFR-ERK1/2-MMP7 signaling pathway induced by dysregulated miRNA-622/197 and their targets LAMC2 and CD82 in gastric cancer. *Cell Death Dis* 8: e2642, 2017.
- Radisky DC, Levy DD, Littlepage LE, Liu H, Nelson CM, Fata JE, Leake D, Godden EL, Albertson DG, Nieto MA, *et al*: Rac1b and reactive oxygen species mediate MMP-3-induced EMT and genomic instability. *Nature* 436: 123-127, 2005.
- Walen KH: Genomic Instability in cancer I: DNA-Repair triggering primitive hereditary 4n-Skewed, amitotic division-system, the culprit in EMT/MET/Metaplasia cancer-concepts. *J Cancer Ther* 9: 974-997, 2018.



This work is licensed under a Creative Commons Attribution-NonCommercial-NoDerivatives 4.0 International (CC BY-NC-ND 4.0) License.